Name: Tat Loon, Chng

MAE 559 Term Paper: Capillary Switches

Table of Contents

Nomenclature

Subscript *A*	Top droplet
Subscript *B*	Bottom droplet
A	Surface area of droplet
E	Potential difference applied to drive electro-osmotic flow
L	Length of electro-osmotic channel
N	Number of electro-osmotic tubes
P	Internal pressure of a droplet
P_{ext}	External or ambient pressure
r	Radius of curvature of the droplet
R_A'	Height of droplet minus its radius of curvature
R_E	Radius of electro-osmotic channel
R_o	Radius of circular orifice
S_o	Reference interfacial energy
S_T	Total interfacial energy of both droplets
T	Switching time of a capillary switch driven by electro-osmosis
U	Net velocity in a channel driven by electro-osmosis
U_P	Smoluchowski velocity attributable to electro-osmosis
U_S	Poiseuille velocity due to capillarity
V_{A-B}	Difference in volumes of droplets A and B
V_o	Volume of a reference sphere with radius R
V_T	Total exposed volume of droplets A and B
β	Minimum non-dimensional pressure required for switch actuation
γ	Surface tension of droplet-air droplet interface
γ^*	Non-dimensionalized surface tension of droplet-air interface for electrochemical technique, γ/γ_w

γ_w	Surface tension of clean water
ε	Permittivity of water
ε_o	Electric constant
ε'	Relative permittivity of water, $\varepsilon/\varepsilon_o$
ζ	Zeta potential of water
μ	Viscosity of water
ρ	Density of water

1. Introduction

A capillary switch can be generally defined as a device in which a capillary surface is manipulated in such a way so as to produce two or more stable states. More specifically, the existence of multiple stable states is implied in the term 'switch' whilst a capillary surface refers to a liquid/gas or immiscible liquid/liquid interface whose geometrical shape is determined by surface tension. For a typical gas/liquid interface such as air and water, the governing length scale (capillary length) occurs on the order of about a millimetre and hence makes such a system an ideal candidate for micro-fluidic devices.

The prerequisites of a sound capillary switch are relatively conventional to the extent of perhaps appearing deceptively simple. These include a straightforward and reliable toggling mechanism, consistent and quick response, and the third which has generated widespread interest of late, being energy efficient.

This paper describes in detail a recently reported approach which not only has the potential of fulfilling all of the above criteria, but whose fundamental operating principle requires reasonably undemanding analysis. These ideas are conveyed in the following section which includes a discussion on the conditions for bistable equilibrium states and the minimum pressure required for switch actuation. Section 3 then elaborates upon three different triggering mechanisms in order of increasing performance. Some potential applications are then discussed in section 4 before the concluding remarks as well as the listing of a few research questions that can be posed as a consequence of this work.

2. Operating principles

a. Bistable static equilibria

We consider the case of two capillary droplets pinned to both the open ends of a circular orifice channel with radius *R* (from here thereof, subscripts A and B are used to denote the top and bottom droplets respectively).

For the sake of simplicity, if we assume that both these droplets adopt a spherical shape of radius *r*, then the pressure difference (Laplace pressure) across the interface of each droplet is given by the Young-Laplace equation:

$$P_A - P_{ext(A)} = \gamma_A \left(\frac{1}{r_{A1}} + \frac{1}{r_{A2}}\right) = {}^{2\gamma_A}/_{r_A} \qquad (1)$$

$$P_B - P_{ext(B)} = \gamma_B \left(\frac{1}{r_{B1}} + \frac{1}{r_{B2}}\right) = {}^{2\gamma_B}/_{r_B} \qquad (2)$$

where *P* is the internal droplet pressure, P_{ext} is the external or ambient pressure, γ is the surface tension between the liquid and the gas (assumed in this paper to be water and air) and *r* is the principal radius of curvature.

If we further neglect gravitational effects and demand the same ambient pressure and interfacial tension, it then follows that if both droplets are to be in static equilibrium, then their radii have to be equivalent ($r_A = r_B$). Figure 1 shows five qualitatively possible equilibrium configurations that can be achieved as a result of this argument. Figures 1a and 1b show respective cases where the total exposed droplet volume, V_T where $V_T = V_A + V_B$ is less than and equal to the reference volume, V_o where $V_o = 4\pi R^3/3$. On the other hand, figures 1c-e present configurations where the total exposed droplet volume is more than V_o.

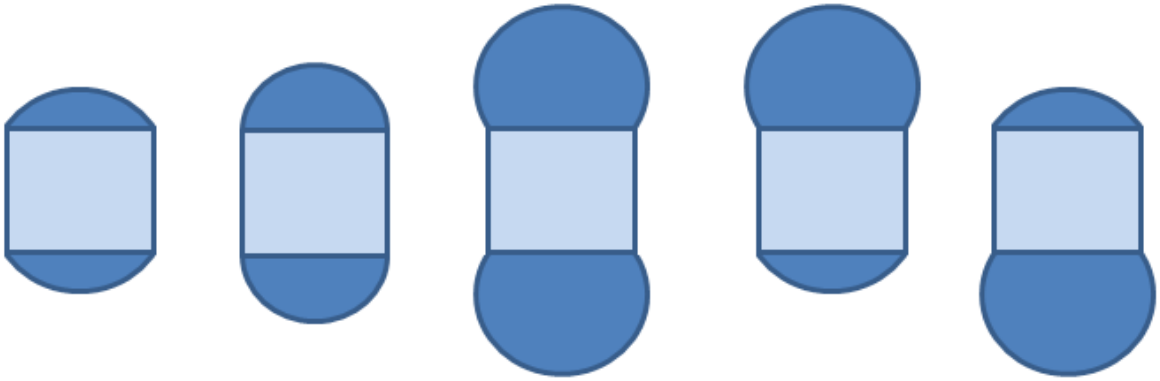

(a) (b) (c) (d) (e)

Figure 1: Various equilibrium configurations ($r_A = r_B$) of a droplet-droplet system. (a): $V_T < V_o$; (b): $V_T = V_o$; (c): $V_T > V_o$ ($V_A = V_B$); (d): $V_T > V_o$ ($V_A > V_B$); (a): $V_T > V_o$ ($V_A < V_B$);

Since the notion of a switch requires that the system must have at least two stable states, then one might intuitively expect that an equivalent volumetric configuration of that in 1d and 1e would be the most eligible of the five listed. This idea can be better understood if we consider one of the droplets in isolation by plotting its Laplace pressure versus its volume. The volume of a single droplet such as that shown in figure 2 can be written as:

$$V_A = \int_{R_A'}^{r_A} \pi x^2 dy = \pi\left[2{r_A}^3/_3 - {r_A}^2 R_A' + {R_A'}^3/_3\right] \; for \; R_A' > 0 \qquad (3)$$

$$= \pi\left[2{r_A}^3/_3 + {r_A}^2 R' - {R_A'}^3/_3\right] \; for \; R_A' < 0$$

where $R_A' = \sqrt{({r_A}^2 - R^2)}$

Both the Laplace pressure and droplet can be non-dimensionalized by $2\gamma/R$ and V_o respectively to give:

$$V_A/V_o = \tfrac{1}{2}\left(r_A/R^3\right) - \tfrac{1}{4}\left(R_A'/R\right)\left[2\left(r_A/R\right)^2 + 1\right] \; for \; R_A' > 0 \qquad (4)$$

$$= \tfrac{1}{2}\left(r_A/R^3\right) + \tfrac{1}{4}\left(R_A'/R\right)\left[2\left(r_A/R\right)^2 + 1\right] \; for \; R_A' < 0.$$

where ${R_A}'/_R = \sqrt{\left[\left({r_A}/_R\right)^2 - 1\right]}$

$$\left(P_A - P_{ext(A)}\right)\Big/_{2\gamma/\mathrm{R}} = \left({R}/_{r_A}\right) \qquad (5)$$

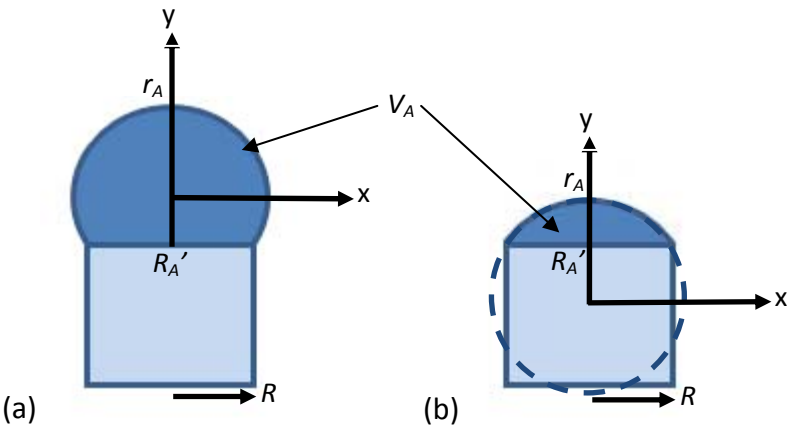

Figure 2: 2D schematic of a single droplet showing the various geometrical quantities in equation (3) (coordinate system adopted is such that origin is at the centre of the droplet). (a): $R_A' < 0$; (b): $R_A' > 0$.

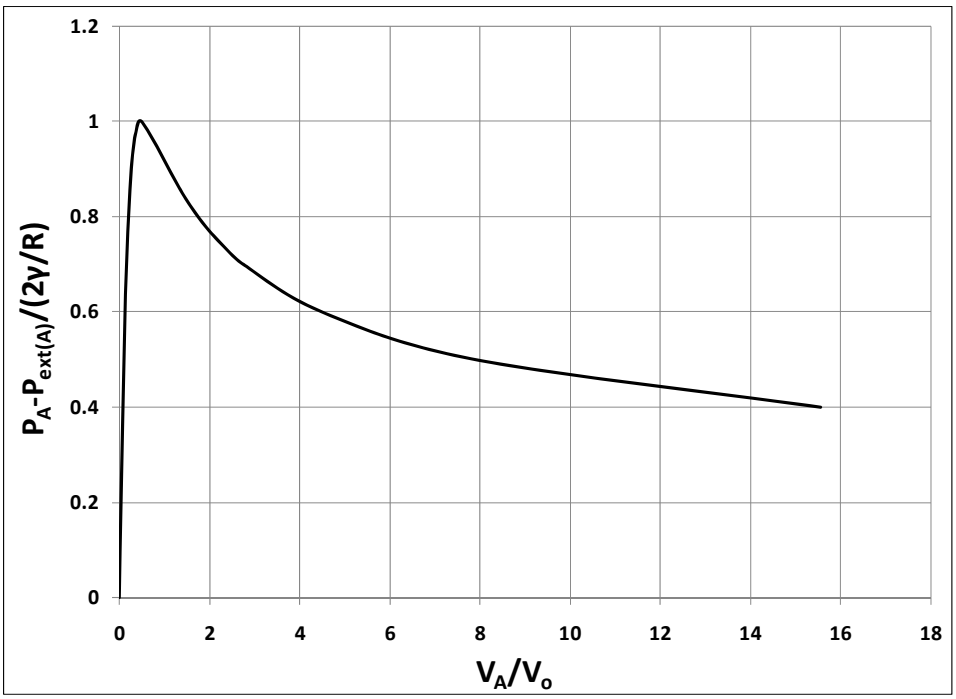

(a)

(b)

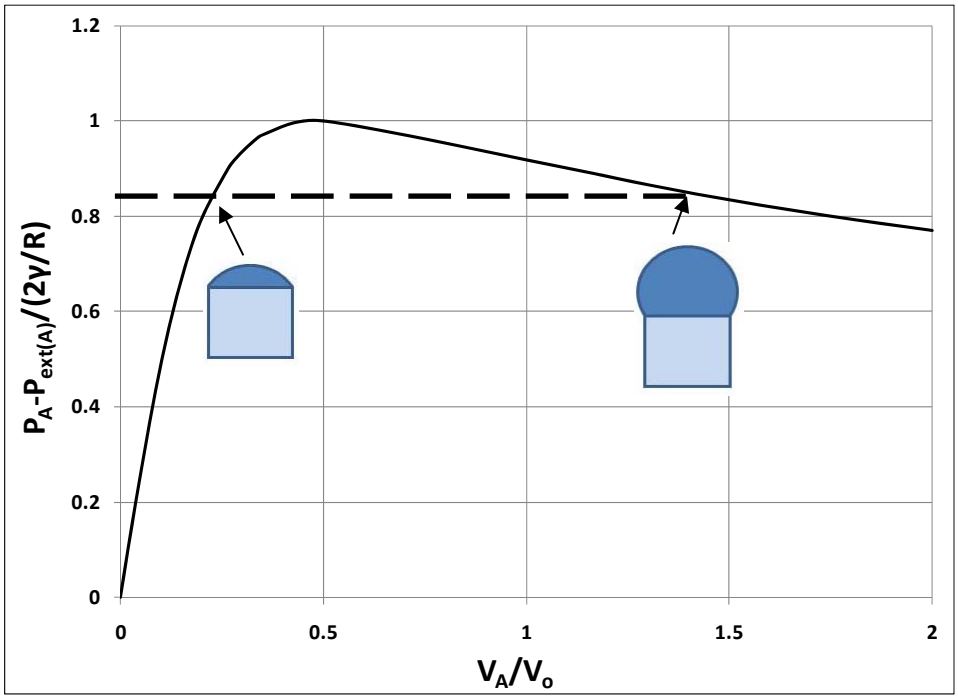

Figure 3: Non-dimensionalized plot of Laplace pressure versus single droplet volume for (a): $0 \leq {}^{V_A}/_{V_o} \leq 20$ and (b): $0 \leq {}^{V_A}/_{V_o} \leq 2.0$ showing that for bistable states to occur, *r/R* must be > 1. (Note that $\left(P_A - P_{ext(A)}\right)/_{2\gamma/\mathrm{R}} = {}^{R}/_{r_A}$)

Equations (4) and (5) clearly show the strong dependence of droplet pressure and volume on the ratio *r/R*. And when viewed together, both these equations and figure 3 further indicate that for bistable states to exist, this ratio must necessarily be more than 1 (the upper limit is discussed shortly). As mentioned, the term bistable refers to the existence of two equilibrium states; with specific reference to figure 3b (see dotted line as an example), a particular value of the Laplace pressure should be capable of supporting two different volume configurations that share the same radius, *r*.

In particular, one also notes that since the pressure depends only on *r/R* whilst the volume scales as $(r/R)^3$, a lower Laplace pressure implies that a much larger volume change is entailed (figure 3a).

Both these ideas can be further illustrated when one considers the difference in droplet volume, $V_{A\text{-}B}$ where $V_{A\text{-}B} = (V_A - V_B)$, plotted against the total droplet volume, V_T. $V_{A\text{-}B}$ is a useful quantity since its absolute value remains invariant at both the static equilibrium states. Figure 4a shows this relationship as well as the corresponding positions of the configurations shown in figure 1. The line in red describes the path of $V_{A\text{-}B}$ when the switch is toggled. Evidently, the criterion for bistability, $r/R > 1$, is re-manifested in the condition that the total droplet volume, V_T must be more than V_o (shaded region of figure 4a). Therefore any choice of total droplet volume, V_T, will in general be capable of functioning as a capillary switch so long as it satisfies $V_T > V_o$ and is not excessively large such that it exceeds the capillary length.

For practical purposes, it is worth noting that for $V_T > V_o$, $|V_{A\text{-}B}|$scales directly with V_T, i.e. the larger the chosen droplet volume, the larger the corresponding volume difference in the two equilibrium states, $V_{A\text{-}B}$. Hence, it would be sensible to choose values of V_T which are not too large. Refs. [1,2] choose a nominal value of $V_T = 2V_o$ in their experiments (see figure 5 for a rough idea of the magnitudes of V_A and V_B at equilibrium).

We briefly mention the special case of the configuration in figure 1c in relation to figure 4a. This case is unique in that it represents an intermediate state which the system achieves as the switch is activated. At the same time, it also appears to satisfy all the conditions required for static equilibrium. However, as we shall see in section 2b, this configuration, as with all those points which lie on the dotted line in figure 4a, correspond to a curve of unstable equilibria based on energy considerations.

As proof of principle, figure 4b shows decent agreement between experimental results[2] and the theoretical curves. The only notable difference is that in their experiments, the authors

imposed an additional net ambient pressure in order to account for the non-negligible influence of gravity.

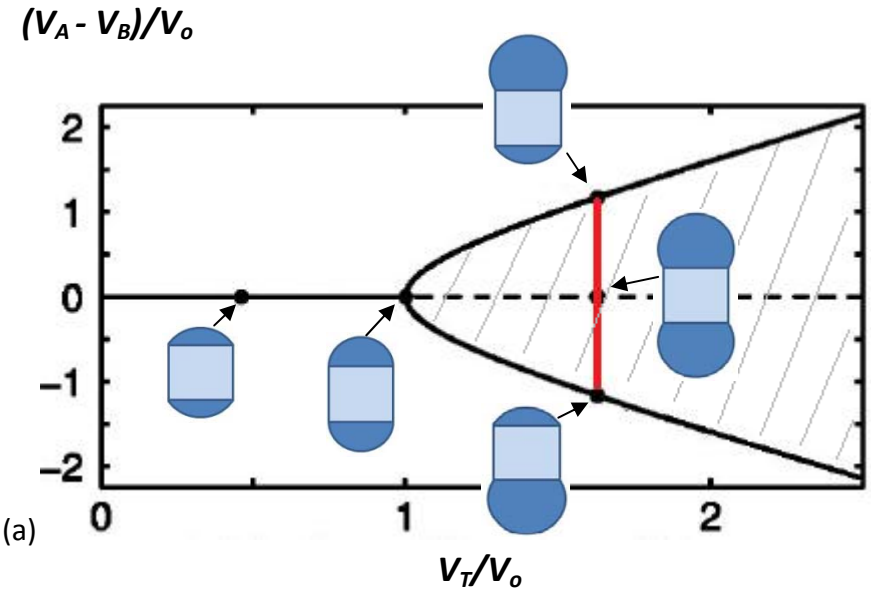

(a)

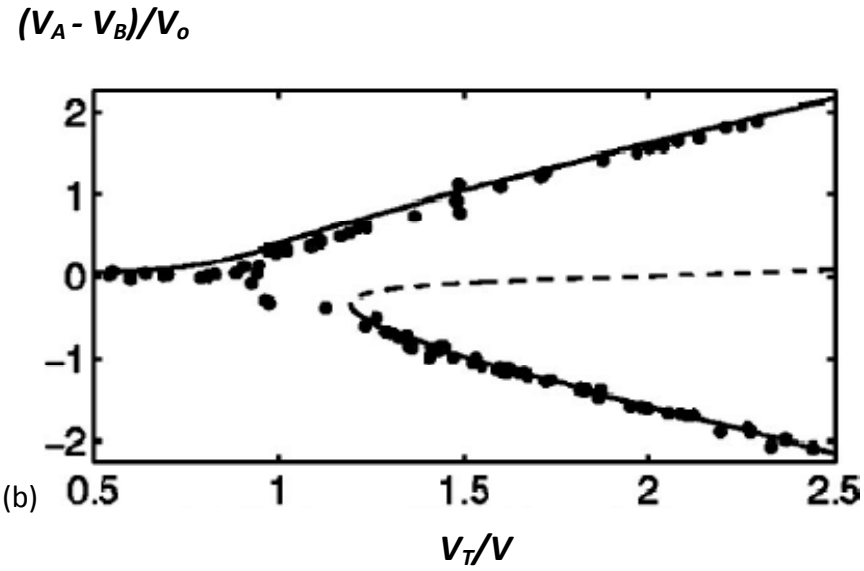

(b)

Figure 4: Plot of droplet volume difference, $V_{A\text{-}B}$, versus total droplet volume, V_T (both non-dimensionalized by the reference volume, V_o). (a): Theoretical curve (modified from ref. [2]); (b) Experimental curve[2].

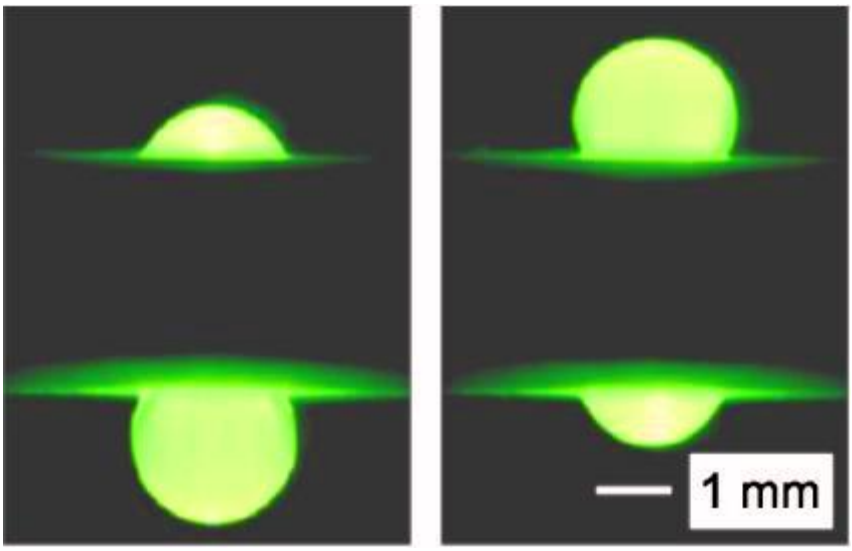

Figure 5: Photographs of capillary switch in both equilibrium configurations[2]. (a): State '0'; (b): State '1'. Fluorescent dye coupled with a laser sheet is used to visualize the flow.

In summary, the foregoing section highlights the relative simplicity of this capillary switch which requires no moving parts and reflects the importance of the geometrical parameter, *r/R* in relation to the problem. From a physical perspective, *R* is the characteristic dimension of the circular channel and *r* can be easily fixed by varying the droplet volume. In a practical application, it is more likely that one would characterize the system through tuning V_T as opposed to *R*.

b. Switch activation (toggling)

Having addressed the criteria for bistable equilibrium, the next logical question one might ask of is to describe the activation process or more specifically, to characterize the intermediate states or behaviour as the switch is toggled.

We can begin elucidating this process by subtracting equation (2) from (1) to arrive at:

$$\Delta P = 2\left(\gamma_A/r_A - \gamma_B/r_B\right) = 2\gamma\left(1/r_A - 1/r_B\right) \qquad (6)$$

where $\Delta P = (P_A - P_B)$ and $\gamma_A = \gamma_B = \gamma$

This equation can be non-dimensionalized by $2\gamma/R$ just as before to give:

$$\Delta P/_{2\gamma/\mathrm{R}} = R\left(1/_{r_A} - 1/_{r_B}\right) \qquad (7)$$

As mentioned in the previous section, if $r_A = r_B$, then $P_A = P_B$ and the system is in equilibrium. However, upon actuation of the switch, this equilibrium is upset and r_A is no longer necessarily equivalent to r_B.

By way of example, let us suppose we have a capillary switch with bistable states '0' and '1' (see figure 5) and a chosen volume V_T such that $V_T = 2V_o$, i.e. $V_A + V_B = 2V_o$. Suppose further that V_A is initially less than V_B, i.e. $V_{A\text{-}B} < 0$, and call this state '0'. If the switch is to be toggled to state '1' where $V_{A\text{-}B} > 0$, then we can analyze this process by tracking the corresponding change in ΔP as $V_{A\text{-}B}$ increases.

Recall that:

$$V_A/_{V_o} = \frac{1}{2}\left(r_A/_{R^3}\right) - \frac{1}{4}\left(R_A'/_R\right)\left[2\left(r_A/_R\right)^2 + 1\right] \; for\; R_A' > 0 \qquad (4)$$

$$= \frac{1}{2}\left(r_A/_{R^3}\right) + \frac{1}{4}\left(R_A'/_R\right)\left[2\left(r_A/_R\right)^2 + 1\right] \; for\; R_A' < 0.$$

Similarly, $$V_B/_{V_o} = \frac{1}{2}\left(r_B/_{R^3}\right) - \frac{1}{4}\left(R_B'/_R\right)\left[2\left(r_B/_R\right)^2 + 1\right] \; for\; R_B' > 0 \qquad (8)$$

$$= \frac{1}{2}\left(r_B/_{R^3}\right) + \frac{1}{4}\left(R_B'/_R\right)\left[2\left(r_B/_R\right)^2 + 1\right] \; for\; R_B' < 0.$$

And from continuity, assuming incompressible flow and no loss of fluid through evaporation, etc:

$$V_T/_{V_o} = (V_A + V_B)/_{V_o} = 2 \qquad (9)$$

Note that at the start since $V_T/V_o = 2$, $r/R = (2)^{1/3}$ and thus $V_{A\text{-}B} = -1.60$. $\Delta P/_{2\gamma/R}$ can be computed by solving for r_A and r_B through the three equations listed above.

Figure 6 shows a plot of this pressure difference versus the droplet volume difference. An immediate inference from this plot is that as $V_{A\text{-}B}$ increases, capillarity first acts to resist the flow ($\Delta P > 0$) but subsequently aids in moving the flow to its other equilibrium state ($\Delta P < 0$). Furthermore, there also exists a certain critical value of ${}^{\Delta P}/_{2\gamma/R} = \beta$ that must be overcome before the switch can be activated. In this example, β is approximately equal to 0.17 but based on the procedure detailed above, one can easily reason that it is in general dependent on the ratio ${}^{V_T}/_{V_o}$. β can hence be thought of as a threshold pressure difference that must be provided externally before the flow can be driven from one equilibrium state to the other.

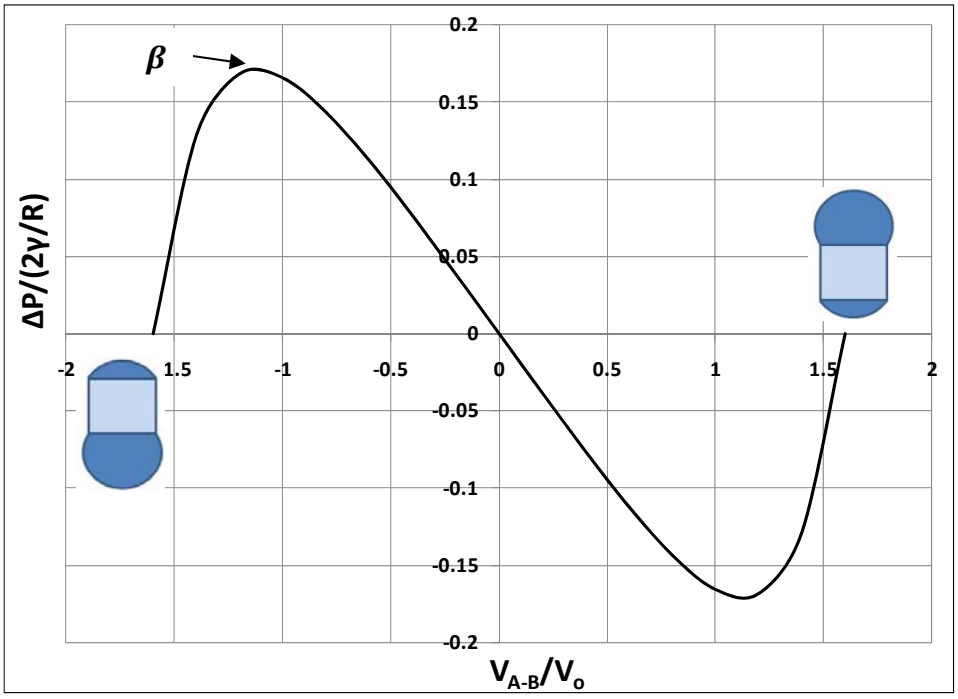

Figure 6: Non-dimensional plot of internal pressure difference between droplets versus difference in droplet volume. The curve exhibits a threshold pressure (non-dimensionalized), β that needs to be provided externally in order to overcome capillarity.

Having defined the external pressure required for the switch to work, a plot of interfacial energy versus $V_{A\text{-}B}$ in figure 7 reveals the respective state that the system will return to if this external driving pressure is suddenly removed. The interfacial energy here is defined as:

$$S_T = \gamma_A A_A + \gamma_B A_B = \gamma(A_A + A_B) \qquad (10)$$

where $A_A = \int_{R_A'}^{r_A} 2\pi x \sqrt{1 + \left(\frac{dx}{dy}\right)^2}\, dy = 2\pi[{r_A}^2 \pm r_A R_A'] \; for \; R_A' \lesseqgtr 0$

and similarly, $A_B = 2\pi[{r_B}^2 \pm r_B R_B'] \; for \; R_B' \lesseqgtr 0$ (refer to figure 2)

(*A* is the droplet surface area and S_T is the total interfacial energy of the system)

S_T can be non-dimensionalized by the reference energy of the system, S_o where $S_o = \gamma(4\pi R^2)$ to give:

$$S_T/S_o = \frac{1}{2}\left[\left(r_A/R\right)^2 \pm \left(r_A/R\right)\left(R_A'/R\right)\right] + \frac{1}{2}\left[\left(r_B/R\right)^2 \pm \left(r_B/R\right)\left(R_B'/R\right)\right] \qquad (11)$$

(Note that the interfacial energy at both equilibria are equal since $r_A = r_B$.)

Since a system perpetually acts to minimize its energy, a point that resides anywhere to the left (right) of the vertical axis will return to state '0' ('1') if the driving pressure is removed. The point where $V_{A\text{-}B} = 0$ is therefore an unstable equilibrium state and corresponds to a configuration analogous to that shown in figure 1c. This can be generalized so that for any particular value of $V_T/V_o > 1$, there will be a corresponding point where $V_{A\text{-}B} = 0$ such as that in figure 7. These form a locus of points corresponding to the dotted line in figure 4a.

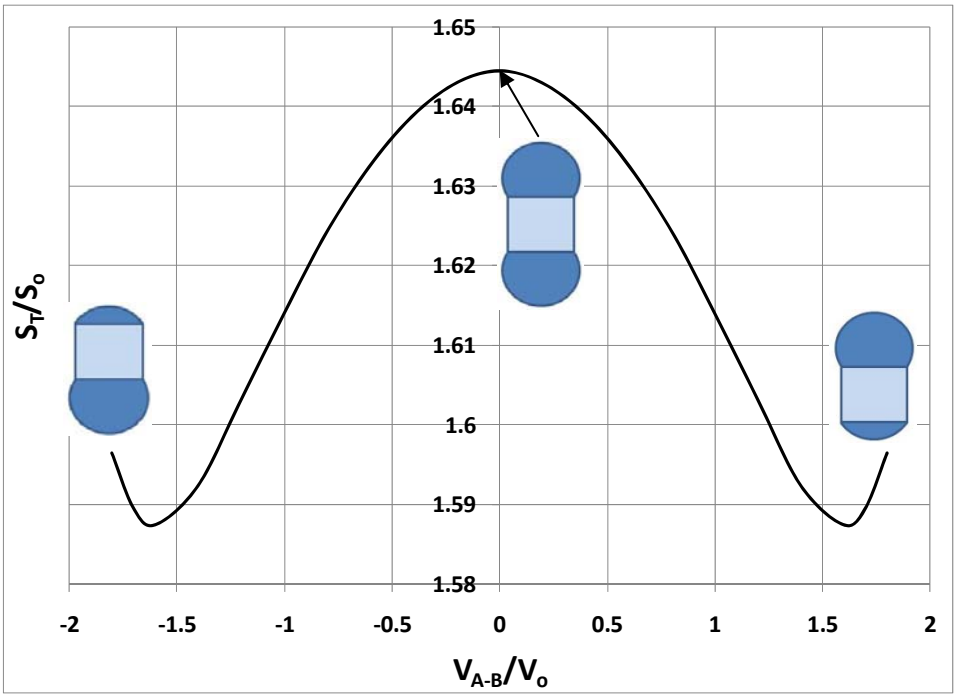

Figure 7: Plot of interfacial energy versus droplet volume difference depicting the stable energy states of the system.

c. **Switching time and energy efficiency**

Two of the reasons that the present device may outperform related designs is its low energy dissipation and the possibility of achieving short switching times. The fact that the underlying geometry involves a triple contact line which is pinned to a solid surface means that the energy dissipation issues associated with designs that involve moving contact lines[3,4] are circumvented. Even then, for viscous dissipation to be avoided, any changes in volume must occur on time scales which are governed primarily by inertia rather than viscosity.

In this connection, non-dimensional analysis defines the inertial and viscous time scales of the problem as $\sqrt{\rho R^3/\gamma}$ and $\mu R/\gamma$ respectively where ρ and μ are the density and dynamic viscosity of the liquid (water) respectively. The ratio of both these scales is therefore given

by $\sqrt{\rho\gamma R}/\mu$ which can be simplified as $\approx 8000\sqrt{R}$ for characteristic properties of water at room temperature This means that for values of *R* on the order of the capillary length, viscous effects occur over much shorter durations and hence acts as a lower limit for the achievable switch time. In particular, for a channel with *R* = 2 mm, the inertial and viscous time scales are 11 ms and 0.03 ms respectively. Remarkably, this means that even if viscous forces are to be avoided, switching times as fast as 11 ms can still possibly be delivered.

3. Triggering Mechanisms

We now turn our attention to possible methods of switch activation. As mentioned previously, switch actuation can essentially be viewed as moving from one equilibrium state to another. For this reason, all triggering mechanisms should somehow effect an inequality in the Young-Laplace equation by introducing a pressure difference so as to overcome β. For this particular problem, based on equations (1) or (2), this is equivalent to either varying the internal droplet pressure, the external ambient pressure or the interfacial (surface) tension. Each of these strategies will be examined in this section.

a. Variation in ambient pressure (pressure pulse)

Arguably the most straightforward of the three, this method entails enclosing the droplet-droplet system in a chamber where the ambient pressure of one or both the droplets can be adjusted. Figure 8 shows a schematic of such a system where the ambient pressure is altered in a pulsed fashion through the use of a stepper motor. The time between successive pressure pulses, which in essence provides a lower bound approximate for the switching time, is about 100 ms.

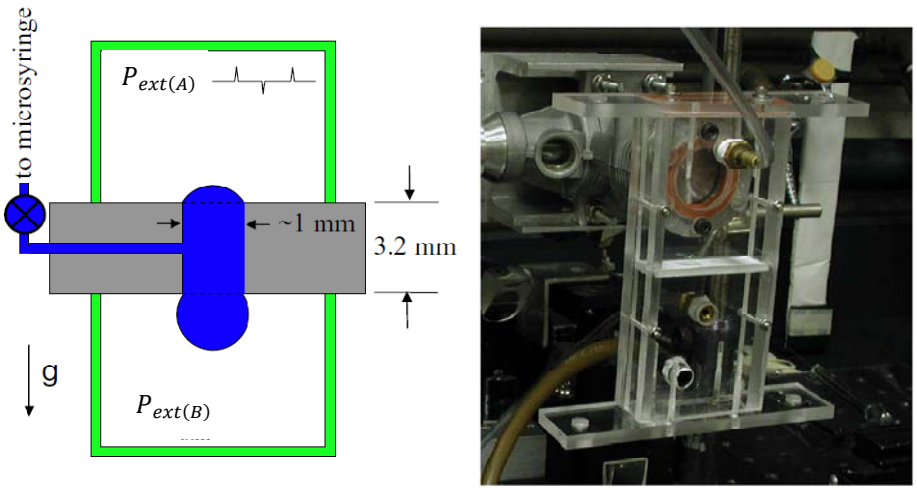

Figure 8: (a): A schematic of a capillary switch that works via a variation in the ambient pressure through the utilization of pressure pulses. (b): Picture of the system. (Note that $P_{ext(B)}$ has to be increased so as to correct for gravitational effects. Graphic source: ref. [5])

However, whilst ostensibly convenient, this method falls short if individual control over a multitude of such switches in a compact environment is desired.

b. Change in surface tension

A plausible way of overcoming the shortcomings of the above approach may be to directly influence the interfacial tensions of the capillary surfaces. To this end, one such method which has found reasonable promise is to use a water soluble surfactant whose surface activity can be controlled electrochemically[1].

By dissolving a suitable amount of this surfactant into the water and applying a small potential difference of 1 V across both ends of the circular channel supporting the two droplets (see figure 9), one can tune the relative surface tension of the two interfaces and hence trigger the switch.

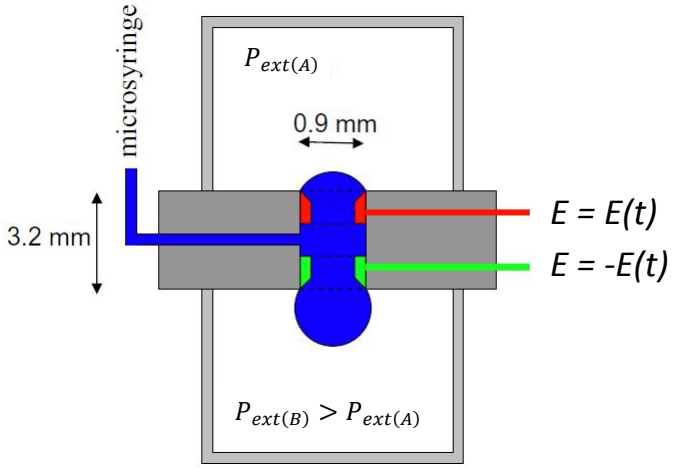

Figure 9: Schematic of a capillary switch that employs a concept of surface tension variation for actuation[5]. A contact path for the potential difference is created by inserting electrically conductive rings at both ends of the circular channel (shaded red and green).

In the presence of a positive electrical potential, the surfactant at that end is oxidized and increases the local surface tension through a reduction in surface activity. As this occurs, there is also a reinforcing effect through an attendant drop in the surface tension at the other end. Figure 10 shows typical experimental results of the difference in droplet volume $V_{A\text{-}B}$ versus total volume, V_T in relation to the theoretical curve shown in figure 4a. These results not only demonstrate the reversibility of this technique but also exhibit promise in that one could envisage lining up an array of these switches in a compact fashion whilst still maintaining full control over their individual states.

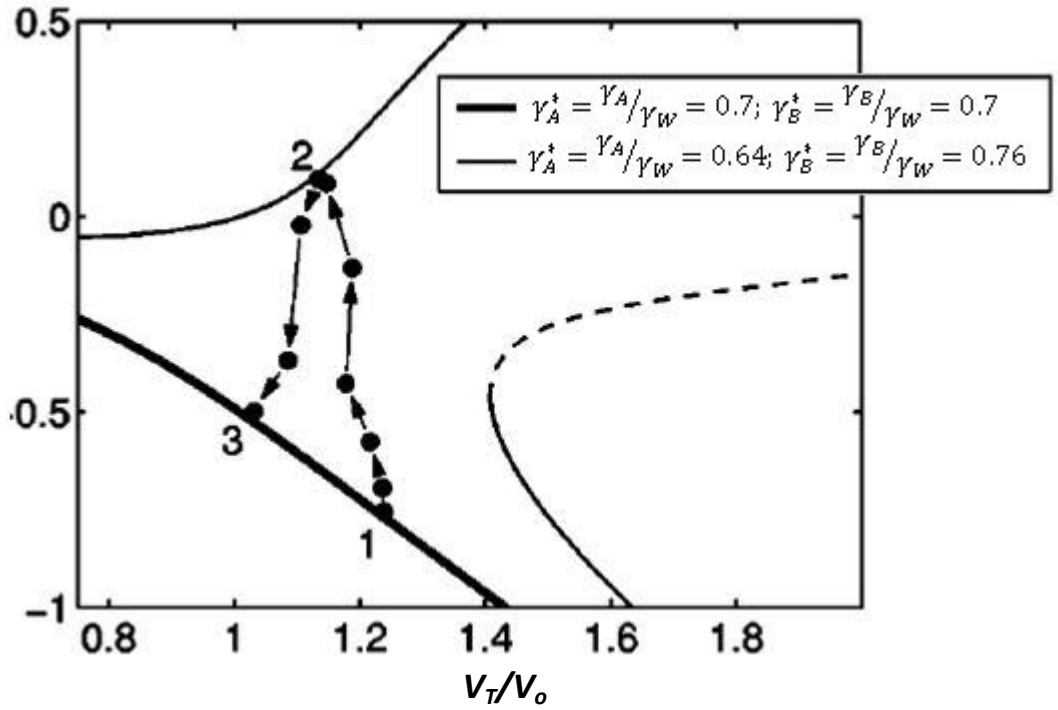

Figure 10: Experimental plot of droplet volume difference, $V_{A\text{-}B}$, versus total droplet volume, V_T for the case where a surface tension variation mechanism is employed (both axes are non-dimensionalized by the reference volume, V_o and γ_W refers to the surface tension of clean water). Note that the change in total volume following a single switching cycle is due to evaporative loss. (Modified from ref. [2])

However, a drawback unique to this method is the slow switch time. The black filled dots in the experimental data of figure 10 correspond to durations of 30 s and the time taken for an entire switching cycle is about 4.5 min.

It is also worth noting that there have been geometrical variants of this approach which have been put forward as prospective optical modulators[3,4]. Figure 11 shows a schematic of such a device and its two operating states. The device consists of mercury liquid which is allowed to flow between two parallel gaps via a small hole. The mercury is surrounded by an electrolyte whose interfacial tension properties with mercury can be modified through an electrical pulse. However, due to the existence of a moving contact line especially in

figure 11b, it is expected that this design would have a higher viscous dissipation as compared to the current device.

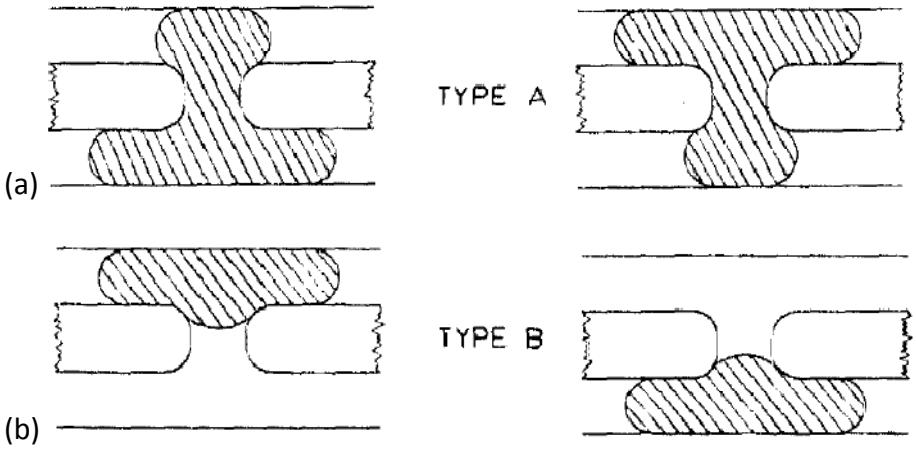

Figure 11: Schematic of an optical modulator design that makes use of electrocapillarity[4].

c. Variation of internal droplet pressure via electro-osmosis

The third triggering strategy, which is the most recent and perhaps effective of the three discussed here, is to integrate some kind of pumping mechanism into the system that can change the internal droplet pressures and hence drive the flow.

To this end, an electro-osmotic pump has been used in ref. [1] with great success. Electro-osmotic flow (EOF) is the motion of liquid induced by an applied potential across a porous material, capillary tube, micro-channel, or any other fluid conduit. As will soon be evident, electro-osmotic velocities, though generally small in magnitude (mm/s), can be made independent of conduit size under prescribed conditions and thus find widespread use in microfluidic applications. EOF is caused by the Coulomb force induced by an electric field on net mobile electric charge in a solution. Though generalizable to other interfaces, the chemical equilibrium between a solid surface and a liquid electrolyte solution typically leads to the interface acquiring a net fixed electrical charge. As such, a layer of mobile ions, termed as an electrical double layer or Debye layer, forms in the region near the interface as shown in figure 12. When an electric field is applied to the fluid (usually via electrodes

placed at inlets and outlets), the net charge in the electrical double layer is induced to move by the resulting Coulomb force.

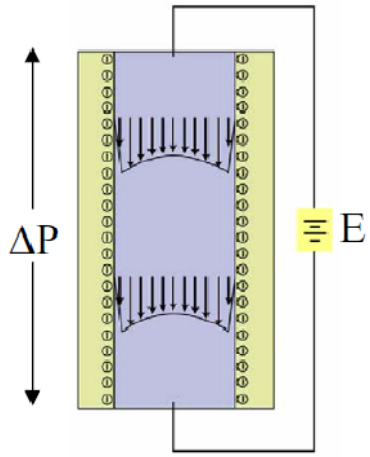

Figure 12: Schematic depicting the phenomenon of electro-osmotic flow[5]. When an electric field (viz. potential difference) is applied parallel to the desired flow direction, the resulting migration of ions formed at the solid/liquid interface leads to liquid motion.

i. Analysis of EOF in a channel

Assuming that the Debye layer is much smaller than the tube dimensions, R_E and L (not to be confused with R the radius of the channel), the velocity in a single tube driven by electro-osmosis is given in the literature by what is known as the Smoluchowski velocity, U_S. The net velocity, however should also take into account the constructive or resistive contribution of the Poiseuille velocity, U_P. The above can thus be written as:

$$U = U_S - U_P \qquad (12)$$

where $U_S = {\varepsilon|\zeta|E}/{\varepsilon_o \mu L}$ and $U_P = {R_E{}^2}/{8\mu}\left({-\Delta P}/{L}\right)$

ε is the liquid permittivity, ε_o is the electric constant, ζ is the zeta potential which provides a gauge of the resulting strength of the Debye layer, E is the applied voltage, L and R_E are the length and radius of the tube respectively.

Not unexpectedly, it follows from the Smoluchowski expression that the velocity generated scales directly with the voltage applied but inversely with the liquid viscosity and channel length. However, what is most unusual is that U_S is independent of the channel radius, R_E (provided the Debye layer condition holds). This fact can then obviously be exploited by choosing appropriately small values of R_E.

Since R_E would then be much smaller than *R*, integrating this mechanism into the current system can be accomplished by utilizing *N* tubes in parallel (see figure 13). This not only provides a simple way of matching the two different geometrical dimensions, but also produces a considerable increase in the flow rate to a level which is of practical use. At microscales, such a concept is easily realizable by choosing a medium of adequate porosity.

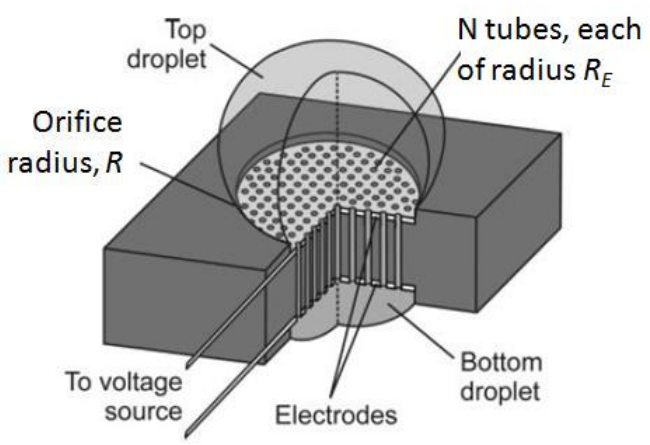

Figure 13: Schematic of an electro-osmotic capillary switch[1].

The corresponding arrangement in figure 13 with *N* tubes can be thought of as *N* electro-osmotic pumps acting in parallel, with each tube (or pump) required to overcome a maximum resistive pressure, β. To further characterize this relationship, we can introduce a non-dimensional variable, *K*, which is the ratio of U_P to U_S, where

$$K = {U_P}/{U_S} = \left[{R_E}^2 \left({\beta\gamma}/{R} \right) \right] \Big/ 8\varepsilon' |\zeta| E = {R_E}^2 \beta\gamma \Big/ 8\varepsilon' |\zeta| ER \qquad (13)$$

and ε' is the relative permittivity of the liquid, $= {\varepsilon}/{\varepsilon_o}$

In the limit of *K* = 1 or more, capillary resistance dominates and there is no flow (i.e. switching does not occur) whilst switching is successful if *K* < 1. A significant inference from equation (13) is that the required voltage, *E* scales as ${{R_E}^2}/{R}$. This favorable scaling implies that any reduction in *R* does not demand additional voltage (power) so long as R_E can be correspondingly decreased.

ii. Switching time for electro-osmotic pump

Assuming negligible changes in density, a first order approximation for the switching time can be computed by dividing the change in volume of the droplet by the volumetric flow rate. The former is simply equal to the value of $V_{A\text{-}B}$ at either of the equilibrium states whilst the latter can be expressed as $N\left(\pi {R_E}^2\right)U$. If we further assume that the Smoluchowski velocity can be made much higher than the Poiseuille velocity (i.e. K >> 1), then an expression for the switching time can be written as:

$$T = {V_{A-B}} \Big/ N\left(\pi {R_E}^2\right) U_S \propto {\mu r^3 L} \Big/ N {R_E}^2 \varepsilon' |\zeta| E \qquad (14)$$

Recalling that (*r/R* > 1 => *r* > *R)* and further excluding material properties, μ, ε', and $|\zeta|$, then we get:

$$T \propto {R^3 L} \Big/ N {R_E}^2 E \qquad (15)$$

An important consequence of the above relationship is that a reduction in *R,* the characteristic length scale of the device, leads to shorter switching times. Furthermore,

since $T \propto {R^3}/{R_E{}^2}$ and $K \propto {R_E{}^2}/{R}$, this means that for shorter switch times, R can be suitably reduced without affecting the system's operating integrity.

4. Applications

Given that a switch is a fundamental element that lies at the heart of almost any sophisticated system, one could presumably envisage a myriad of applications for the current device. Two particular applications have been put forward by ref. [1], namely as an adhesion device as well as a particle mover.

The adhesion device (see figure 14) would simply comprise of a series of capillary switches, which when activated in unison, produces a significant adhesion strength sufficient to lift an object. Harnessing the synergistic capabilities of an array of these switches has its motivations in the palm beetle which uses a similar idea to attach itself onto a palm leaf when defending itself against attacking ants[6]. In particular, the authors in ref. [1] make a remark on the palm beetle 'It is this combination of reversibility and strength that is most remarkable (man-made bonds, such as epoxy, are stronger but not easily reversed).'

For a simple device like a reversible adhesion pad, the straightforward pressure pulse approach would probably lend itself to greatest use since individual controllability of the switches is not critical.

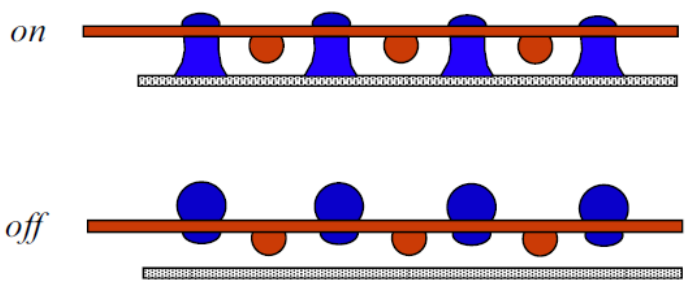

Figure 14: Cartoon showing the proposed working concept of an adhesion device that utilizes multiple capillary switches.

The particle mover, as the term implies, refers to a device that is capable of delivering a particle from one desired location to another. Figure 15 shows two possible approaches that could be employed. The general idea does not differ much from the adhesion device except for the fact that individual addressability of the switches and the switching time is probably more crucial.

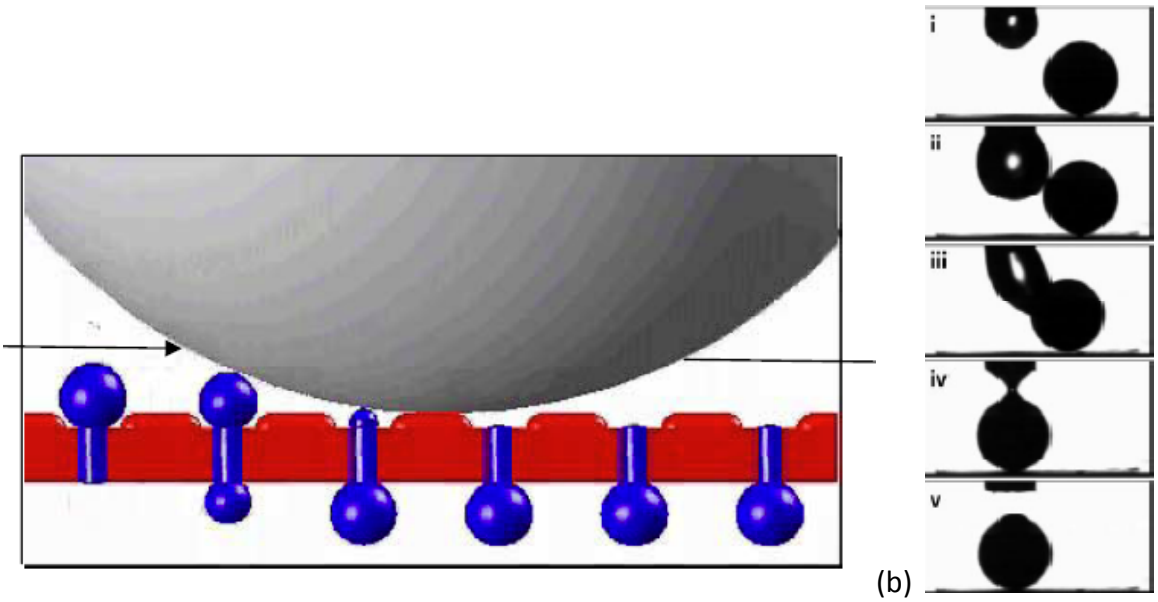

(a) (b)

Figure 15: (a) Cartoon showing the working concept of a particle mover[5]; (b) Sequential images of a capillary switch functioning as a particle mover[1]. Another capillary switch accurately positioned to the left would move the particle if the same sequence is repeated.

A third application that may offer consequent promise is a surface with dual properties. By characterizing and combining two immiscible liquids within the switch, one may imagine creating a surface that can 'toggle' between properties of either liquid.

As regards all the above applications, a less volatile liquid could be chosen so as to minimize evaporative loss in instances where the choice of working fluid is deemed not to be critical.

5. Concluding remarks

The working principles and main actuation mechanisms of a capillary switch have been duly discussed in this paper, together with some ideas for its practical application. In its most

basic form, the device consists of two droplets of liquid pinned to a circular orifice, an arrangement that minimizes viscous dissipation due to the stationary contact line.

The geometric ratio of the droplet to channel radius (*r/R)* is shown to be important for the existence of bistable states as well as for determining the minimum pressure necessary for switch actuation. Triggering mechanisms can also be categorized according to the different terms that constitute the Young-Laplace equation. These include a variation in ambient pressure, surface tension as well as internal droplet pressure. Specific mention is reserved for an electro-osmotic technique which involves the latter and has been experimentally proven to yield consistent toggling response and short switching times.

6. Future work

Indeed, the capillary switch is an ingenious application which presents thought provoking questions not just in relation to issues regarding its future application but also for scientific research.

For robust operation, the choice of working fluid to complement the intended target surface can become extremely critical and perhaps challenging. This will require characterization of their interfacial properties so as to minimize or even **control** the residual fluid that is left on the contacting surface. Theoretical models may also be required to understand the dynamical effects of the system, for example, as it oscillates before returning to its respective equilibrium states. This has been partially addressed in refs. [7, 8].

Finally, one may also question if a system of such a nature with more than two stable states can exist, see for instance schematics in figure 16. In this connection, admitting a variation in radius of the geometry may also introduce desirable changes in stability (figure 16b).

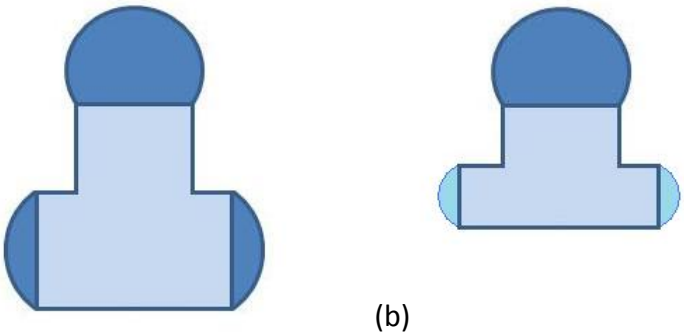

(a) (b)

Figure 16: Schematics of possible capillary switch concepts with more than 2 stable states (b): With two different working liquids.

References:

1. Vogel, M. J., Ehrhard, P. and Steen, P. H., 2005, “The Electroosmotic Droplet Switch,” Proc. Natl. Acad. Sci. USA, Vol. 102, No. 34, pp. 11974-11979.
2. Hirsa, A. H., Lopez, C. A., Laytin, M. A., Vogel, M. J. and Steen, P. H., 2005, “Low-dissipation Capillary Switches at Small Scales,” Appl. Phys. Lett., Vol. 86, 014106.
3. Lea, M., 1983, “An Optical Modulator Based on Electrocapillarity,” Appl. Phys. Lett., Vol. 43, No. 8, pp. 738 - 740.
4. Lea, M., 1985, “Static Stability of Mercury Mirror Light Modulators,” J. Appl. Phys., Vol. 58, No. 1, pp. 108-114.
5. Steen, P. H., Bhandar, A., Vogel, M. J. and Hirsa, A. H., 2004, “Dynamics and Stability of Capillary Surfaces: Low-dissipation Liquid Switches,” NASA/CP-2004-213205, Vol. 2.
6. Eisner, T. and Aneshansley, D. J., 2000, “Defence by Foot Adhesion in a Beetle (Hemisphaerota Cyanea),” Proc. Natl. Acad. Sci. USA, Vol. 97, No. 12, pp. 6568-6573.
7. Slater, D. M., Lopez, C. A., Hirsa, A. H. and Steen, P. H., 2008, “Chaotic Motions of a Forced Droplet-droplet Oscillator,” Phys. Fluids, Vol. 20, pp. 092107.

8. Bostwick, J. B. And Steen, P. H., 2009, “Capillary Oscillations of a Constrained Liquid Drop,” Phys. Fluids, Vol. 21, pp. 032108.

Attachments:

(Document should be viewed with 4 supporting videos)